©2016

Robert Weir

ALL RIGHTS RESERVED

HOLLOW JANUS CYLINDERS AT LIQUID INTERFACES

By

ROBERT ERIC WEIR

A thesis submitted to

the Graduate School-New Brunswick

Rutgers, The State University of New Jersey

In partial fulfillment of the requirements

For the degree of

Master of Science

Graduate Program in Mechanical Engineering

Written under the direction of

Shahab Shojaei-Zadeh

And approved by

_____

_____

_____

New Brunswick, New Jersey

May, 2016

ABSTRACT OF THE THESIS

Hollow Janus Cylinders at Liquid Interfaces

by ROBERT WEIR

Thesis Director:

Shahab Shojaei-Zadeh

In this dissertation, capillary-induced interactions and self-assembly behavior of amphiphilic hollow Janus cylinders at an air-water interface is numerically investigated. First, preferred orientation of a single hollow Janus cylinder is determined as a function of amphiphilicity and aspect ratio. When the cylinder is horizontal (long axis parallel to the interface), the shape of the deformed interface and the resulting capillary-induced interactions between a pair of cylinders is examined. In addition, preferred tip-to-tip or side-by-side assembly behavior of a pair of cylinders is determined by minimizing the total interfacial energy of the system. The preferred assembly behavior of a pair of hollow Janus cylinders is side-by-side for higher amphiphilicities, but as the amphiphilicity is reduced, tip-to-tip orientation becomes similarly preferable. The case of hollow Janus cylinders is also compared with their homogeneous counterparts as well as with solid homogeneous and solid Janus cylinders. The significant difference between Janus and homogeneous hollow cylinders is that the preferred orientation of a homogeneous hollow cylinder is horizontal with respect to the interface for given contact

angles and at large aspect ratios. Meanwhile hollow Janus cylinders with large aspect ratios and amphiphilicities ($\beta \geq 20$) prefer a vertical orientation (piercing the interface). The preferred orientation of a single solid Janus cylinder behaves similarly to its hollow counterpart except it prefers a vertical orientation at higher amphiphilicities. In comparison, single hollow and solid homogeneous cylinders have almost similar preferred orientation. The outcome of this study may provide insight on self-assembly behavior of model hollow particles, such as carbon nanotubes, at liquid interfaces for fabrication of functional monolayers or for use as interface stabilizers in foam and emulsions.

.

Acknowledgements

First, I would like to thank my advisor, Dr. Shahab Shojaei-Zadeh for allowing me to conduct research under his tutelage. He pushed me in all the right directions and without his help I would have never finished my M.S studies. I also want to thank my thesis committee members, Dr. Drazer and Dr. Diez for reviewing my thesis.

I want to thank Dr. German Drazer for his support and insight on research during our group meetings. I am grateful to Dr. Hossein Rezvantalab and Dr. Ken Brakke for their help with my Surface Evolver code. I also want to thank my lab-mates and group members for all their support over the years: Stephen Rowe, Siqi Du, Tianya Yin, David Cunningham, and Isabel Liberis.

I want to thank my parents for supporting me during my time at Rutgers, without them I would have never made it this far. They allowed me to focus on my studies and succeed to the best of my abilities. Lastly, I want to thank my girlfriend, Jeanine for supporting me and putting up with all of my long hours of work. Without her I would have never been able to complete this degree.

Table of Contents

Contents

List of Illustrations

Chapter 1

Introduction

1. Introduction

1.1 Janus Particles

The idea of Janus particles were first introduced by De Gennes in 1991.[2] These particles were named after the roman god Janus, who is depicted as having two faces. De Gennes observed that particles with two different sides of wettability uniquely aggregate at an interface. Janus particles are unique among particles, due to their asymmetric surface properties they can self-assemble into complex structures.[1] A wide variety of different geometries of Janus particles have been fabricated, as shown in figure 1. While

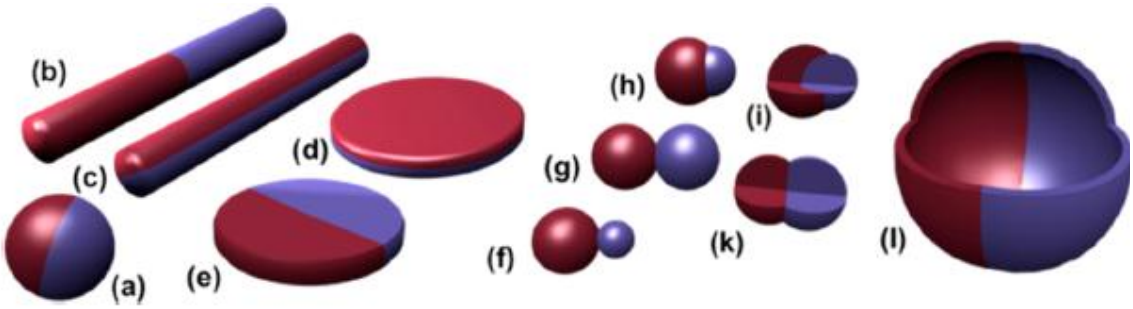

Figure 1 – Different shapes of Janus particles, (a) spherical, (b,c) cylindrical, (d,e) disc-shaped, and (f-l) various dumbbell-shaped Janus particles.[1]

most of our focus is on Janus particles with different wetabilities, they may also be asymmetric with respect to electrical, magnetic, optical, and catalytic properties. Due to their versatile characteristics, Janus particles have already been used in optical probes, drug carriers, and emulsion stabilizers.[3, 4, 5, 6, 7, 8]

1.2 Particles at an Interface

Two of the most important properties of Janus particles are their ability to self-assemble into complex monolayers and their ability to stabilize foams and emulsions by adsorption at liquid-fluid interfaces. Controlled self-assembly at an interface of Janus spheres, cylinders and discs was first observed by Müller et al..[9, 10, 11, 12, 13] This led to more in-depth looks at the mechanics of how these Janus particles self-assemble. Janus particles have also been shown to assemble in bulk fluids as well.[14, 15, 16, 17]

Foam and emulsion stability is a research area that has been extensively studied due to the considerable importance of properties such as functionality and shelf life of these complex fluids, which depend on their ability to remain phase-separated. Conventionally, surfactants have been used as stabilizers, as they adsorb to the interfaces between the dispersed and continuous phases and increase the kinetic stability of the substances by providing steric and electrostatic repulsion between dispersed phase droplets.[18] Surfactant molecules exhibit equilibrium between the interface and the bulk.[19] Another method of stabilization is the use of solid particles instead of surfactants. Colloidal particles at a fluid-fluid interface work similarly to surfactants and are harder to detach from the interface; their adsorption is effectively irreversible in nature.[20] Spherical and cylindrical particles in particular have been the focus of research in particle stabilization of foams and emulsions. Micrometer sized spherical particles attached to an oil-water interface remain stable against thermal fluctuations;[21] the long range capillary attraction between these particles can also be tuned by an electrostatic field.[22] Spherical particles at an air-water interface exhibit spontaneous assembly into meso-structures,[23, 24, 25, 26, 27] while solid cylinders spontaneously assemble into a tip-to-tip orientation and form

rigid straight chains.[28] The capillary force between these cylinders can be calculated by using their translational and angular velocity to satisfy force and torque balances.[29] Research has also been done on numerical models studying the assembly of vertical cylinders piercing an interface and the interface deformation due to these cylinders.[30, 31]

Though homogeneous particles engender better stability in foams and emulsions than do surfactants, they are still only kinetically stable, since the free energy of formation is positive.[32] Recently, anisotropic particles have been shown (theoretically) to create thermodynamically stable emulsions, which would significantly increase the longevity of these complex fluids.[33] Anisotropy in particles can include patchiness, aspect ratio, and faceting.[34]

Various geometries of Janus particles have been studied to help increase stabilization of foams and emulsions. In general, the preferred orientation of Janus particles at an interface depends on particle shape, aspect ratio and surface chemistry.[35] The most commonly studied shape of Janus particle is spherical. Several works have investigated the equilibrium orientation and capillary interactions between Janus spheres.[19, 35, 36, 37, 38, 39, 40] A Janus sphere at an interface prefers to orient itself in such a way that each area on the particle is wet by its favorite fluid.[37, 38, 40] Janus ellipsoids have preferred orientation that depends on the particle aspect ratio and hydrophobicity.[41] Solid Janus cylinders can have a preferred orientation similar to that of a sphere, where each area is wet by its favorite fluid, or to that of an ellipsoid, where it is tilted at the interface; the observed behavior depends on the aspect ratio of the cylinder.[42]

1.3 Current Research

In the present work we introduce a new class of particle, hollow Janus cylinders. We investigate the interfacial deformations caused by homogeneous and hollow Janus cylinders and homogeneous and solid Janus cylinders at an air-water interface. The interface is deformed due to a combined effect of surface wettability and geometry. We calculate the surface tension of neighboring fluids and the area wet by each of the fluids to solve for the interfacial energy. We then characterize the attraction and repulsion of a pair of cylinders at an air-water interface. By doing so, we can determine maximum distance of interaction and how they prefer to assemble. We use this interfacial energy to determine the preferred orientation by varying the angle φ between the two cylinders and computing the interfacial energy of each configuration; the angle that minimizes this energy corresponds to the preferred orientation.

This thesis is organized as follows: In chapter 2, we discuss our model and simulation methodology. In chapter 3 we discuss the results of hollow homogeneous cylinders at an air-water. In chapter 4 we focus on solid homogeneous cylinders and how they compare to hollow cylinders. In chapter 5 we investigate the interactions of hollow Janus cylinders, and finally in chapter 6 we compare these hollow Janus cylinders to solid Janus cylinders. In each of these sections we focus on the preferred orientation of single cylinders and the interaction between pairs of cylinders. In chapter 7 we summarize the results and the implications of our work.

Chapter 2

Simulation Method

2. Simulation Method

We use Surface Evolver to investigate interface deformation and capillary interactions between hollow cylinders at an air-water interface. This FEM program has been used to investigate capillary interactions between Janus and patchy particles at an interface.[35, 43, 44] Surface evolver uses different optimization methods such gradient descent, hessian matrix, and conjugate gradient to study surfaces shaped by forces and constraints.[43] While we use Surface Evolver to study particles at an interface, it can also be used for modeling of soap bubbles, foams and liquid solder.[43]

Models are set up so the first step is to define vertices in your domain box. Vertices are defined by giving them coordinates in the x, y, and z plane. These vertices able to be constrained based on your system. Vertices are the basis of all of the models in

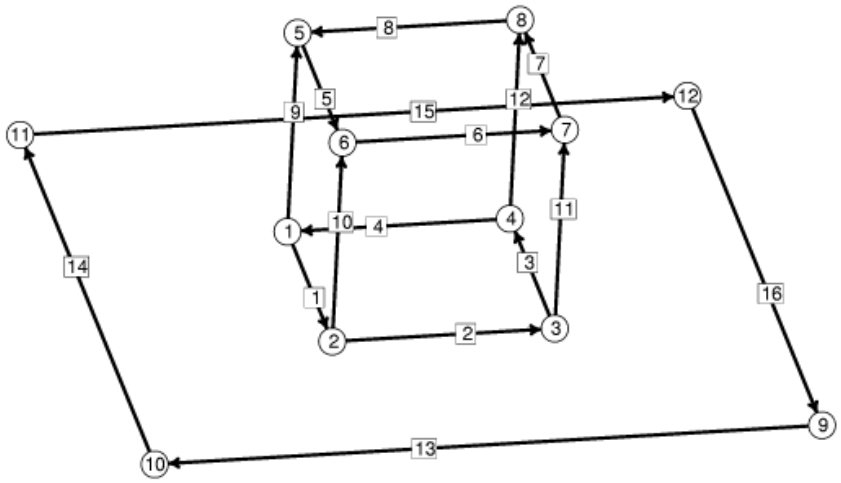

Figure 2 – Schematic of a droplet on a substrate in Surface Evolver. The numbers in the circles represent the vertices and the numbers in the squares represent the edges.

surface evolver, which make up the core of our simulations. Once all of the vertices have been placed into the model, the next step is to connect them via edges. Edges are connected between two vertices and start to create the initial geometry. Constraints are applied similarly to edges as they were vertices. Finally groups of edges are connected together to create the facets of the model. These facets are where the surface tension is defined. An example of a droplet on a substrate is shown in Figure 2. In this example edges 13-14-15-16 are connected into one face, which represent the surface that the droplet is sitting on. The surface is set using the "fix" command on the vertices, edges and facet. This command removes the variable of deformation and movement of the surface. The droplet is defined by using 6 facets as shown in Figure 2. Only one of the facets is in contact with the solid surface, the rest are in contact with air. To set these characteristics, each facet must be specified a surface tension with whatever it is adjacent to. The five facets in contact with air will be specified with water-air surface tension, the facet in contact with the surface will be specified based on the contact angle. Once the vertices, edges, facets and all their constraints are specified, we can add in volume of our liquid, gravity and density, depending on what our simulation calls for.

Once the model is completed, you may begin the refinement code. The refinement code needs to be changed for every model. This code is used to make our models approach their minimum energetic state. If we run our refinement code on the droplet on a substrate the cube with deform to the minimum energetic state; which looks like a droplet as shown in figure 3. One of the most common refinement commands is "r", which refines the triangulation of your model. The command "g" is the input for gradient descent iterations, "V" is vertex averaging which computes the new position of the

vertices based on adjacent faces, “u” is equiangulation which polishes up the triangulation of the model, and “U” is used to turn on conjugate gradient mode.

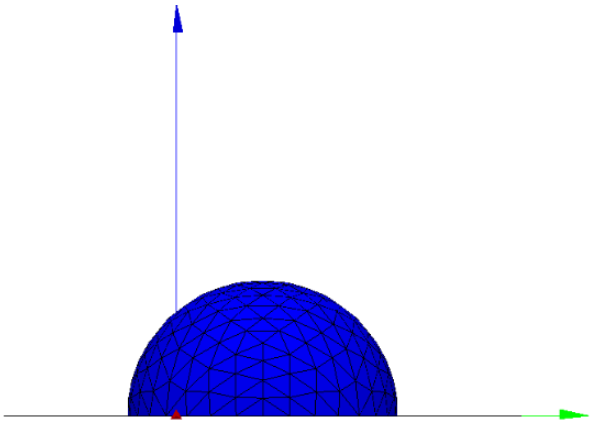

Figure 3 – Droplet evolved using surface evolver refinement code based on the model in figure 2.

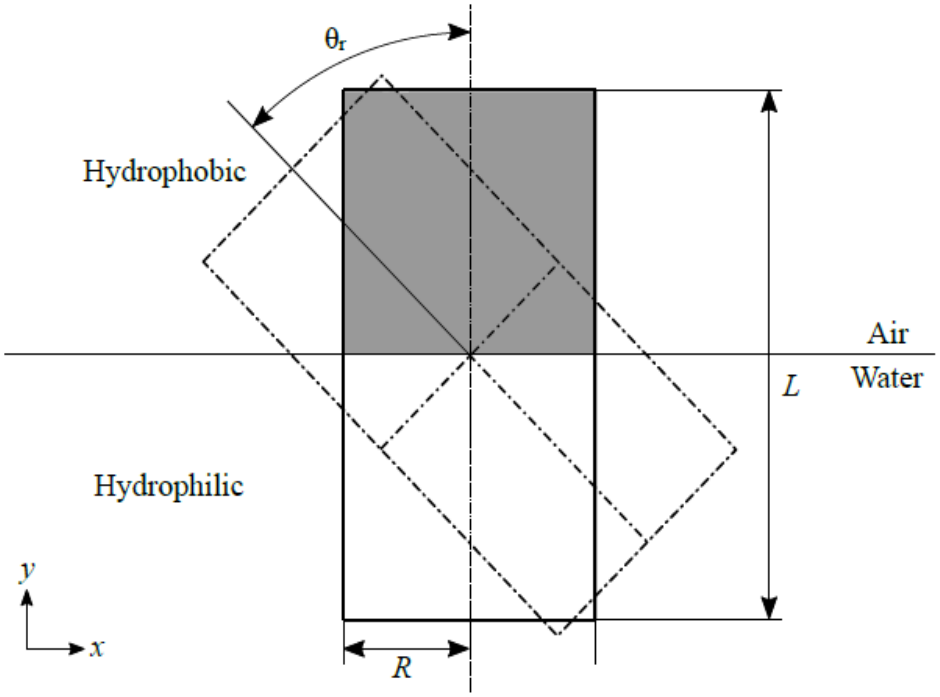

Figure 4 – Schematic of a Janus cylinder (hollow or solid) tilting about the interface measured with angle θ_r from the vertical direction.

After explaining how surface evolver works we turn our attention to how Janus cylinders are created in Surface Evolver. A Janus Cylinder is placed in predefined orientation based on cylinder geometry and surface wettability. The Janus cylinder will deform the interface to satisfy wetting conditions. Surface Evolver finds the deformation profile by calculating the minimum surface energy of the system. The optimization methods include gradient descent and conjugate gradient.

Single cylinders are rotated around the z-axis as seen in figure 4. The geometric parameters include cylinder length L, outer radius R, and orientation angle θ_r. The orientation angle ranges from 0° to 90°, where 0° corresponds to vertical and 90° to horizontal orientation. For hollow Janus cylinders, amphiphilicity, the difference between the hydrophobic and hydrophilic contact angles, is described by β as:

$$\theta_{Hydrophobic} = 90° + \beta$$
$$\theta_{Hydrophillic} = 90° - \beta \quad (1)$$

The aspect ratio AR of the cylinder is defined as the ratio of the length to outer radius, $AR = L/R$. The total interfacial energy of the hollow and solid Janus cylinders is described as:

$$E = \gamma_{aA}A_{aA} + \gamma_{pA}A_{pA} + \gamma_{pW}A_{pW} + \gamma_{pW}A_{pW} + \gamma_{AW}A_{AW} \quad (2)$$

Where E represents the total surface energy, γ represents the interfacial tension, and A represents the area wetted by a designated fluid. The subscripts a and p represent the hydrophilic and hydrophobic areas of the cylinder. The subscripts A and W represent the

air and water phases, respectively. The areas wetted by fluids include inside, outside, front and rear face of the cylinder.

To find out the preferred position *H* (with respect to the interface) of a Janus cylinder at θ_r = 90°, we let the cylinder move in the y-direction, as shown in figure 5. The outer boundary of the interface is pinned to allow the interface to deform around the cylinders. This process allows us to determine the preferred position of the cylinder as a function of contact angle.

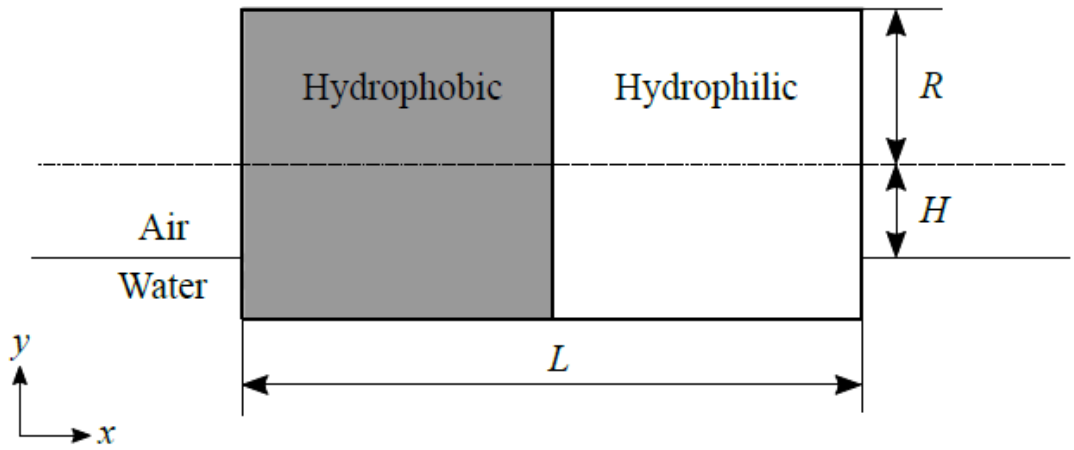

Figure 5 – Schematic of the position of the center of the hollow Janus cylinder (*H*) with respect to the interface.

Pairs of homogeneous and Janus cylinders are placed at the interface and are separated from each other by $d_{cc,}$ their center-to-center distance. The separation distance between the cylinders after which they no longer interact with each other via capillary interactions is used to nondimensionalize the capillary energy as:

$$E_{Capillary} = \frac{E - E_f}{\gamma RL} \tag{4}$$

where E is the interfacial energy at a given spacing, and E_f is the interfacial energy when cylinders are far apart and do not interact with each other, and R and L are the outer radius and length of the cylinders, respectively.

To determine the preferred assembly orientation of a pair of cylinders at the interface, we minimize their interfacial energy as they approach each other with angle φ, as shown in figure 6. This angle ranges from 0° for side-by-side to 180° for tip-to-tip orientation.

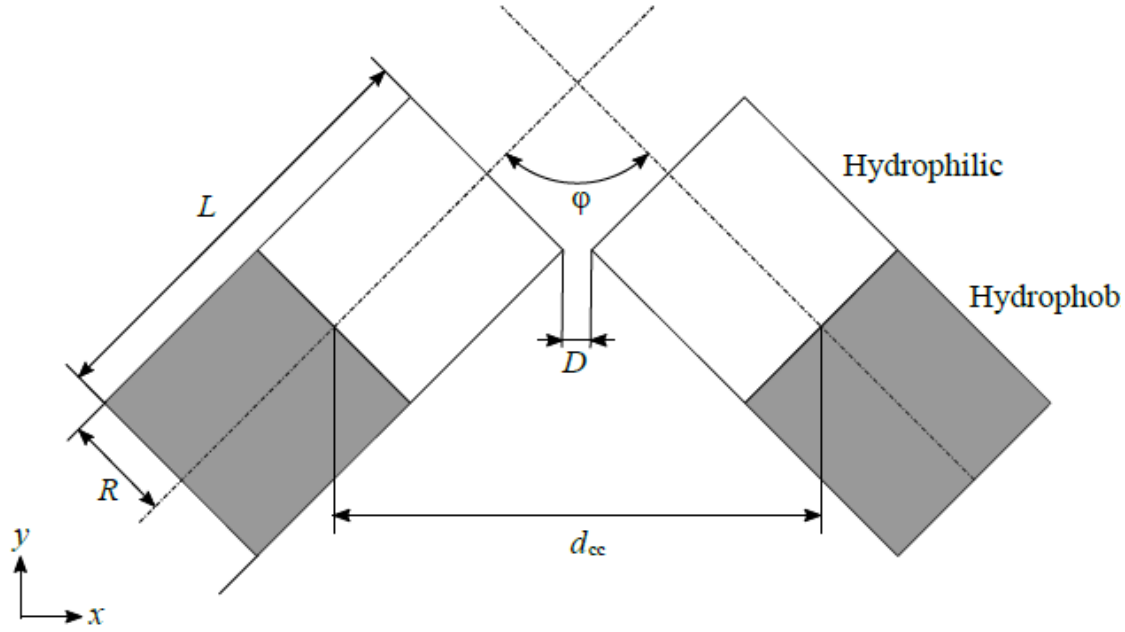

Figure 6 – Top-view schematic of two interacting hollow Janus cylinders used to determine their preferred in-plane orientation.

Chapter 3

Hollow Homogeneous Cylinders

3. Homogeneous Hollow Cylinders

We begin by examining the preferred orientation of a single homogeneous hollow cylinder. The cylinder is rotated about the interface as seen in figure 4 and its preferred orientation is a function of aspect ratio and contact angle. We vary aspect ratio from AR = 1 to AR = 10 and use three different contact angles, θ = 30, 80, 150°. From the results shown in figure 7, we observe that for a contact angle of 30° and aspect ratios less than 3 the cylinder prefers an orientation angle of 0°(vertical to the interface). At larger aspect ratios, orientation angle of 90°(parallel to the interface) is preferred. Similarly, for contact

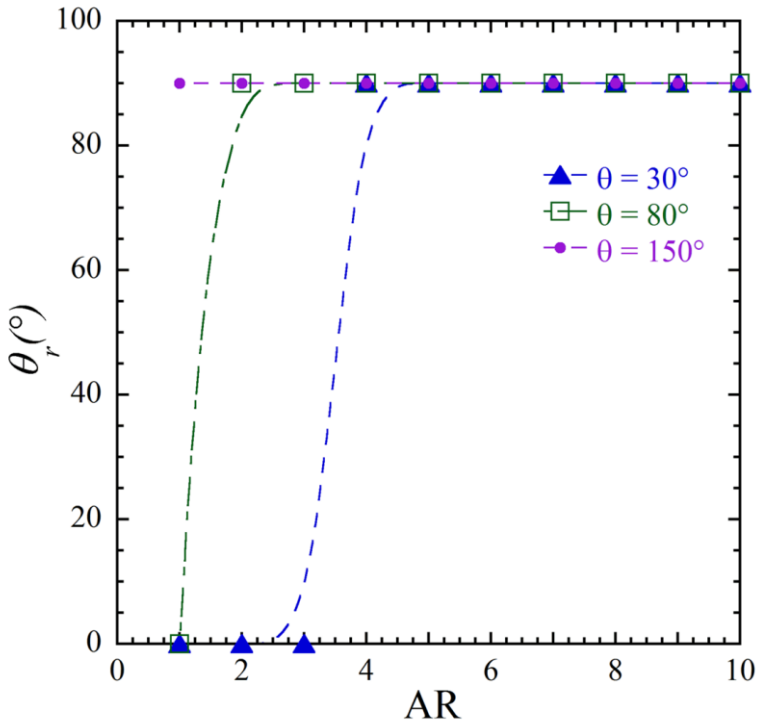

Figure 7 – Orientation as a function of aspect ratio for a single homogeneous hollow cylinder with contact angle θ = 30, 80, and 150°.

angle of 80°, the cylinder prefers a horizontal orientation for AR ≤ 1 and a vertical orientation for AR > 1. For contact angle of 150° the cylinder prefers an orientation angle of 90° regardless of the aspect ratio.

The preferred position of a hollow homogeneous cylinder parallel to the interface is investigated. Three different contact angles of 30, 80, and 150° and aspect ratio of 5 is considered. The edges of the interface are pinned in the domain box and the cylinder is free to move up and down so that the interface around the cylinder can deform to minimize the interfacial energy. The results from varying the height *H* of the cylinders with different contact angles can be seen in figure 8. At a hydrophobic contact angle of 150°, the cylinder prefers to sit on top of the interface at *H/R* = -1.0 as water does not get into the hollow cylinder. At a hydrophilic contact angle of 30° the cylinder prefers to sit

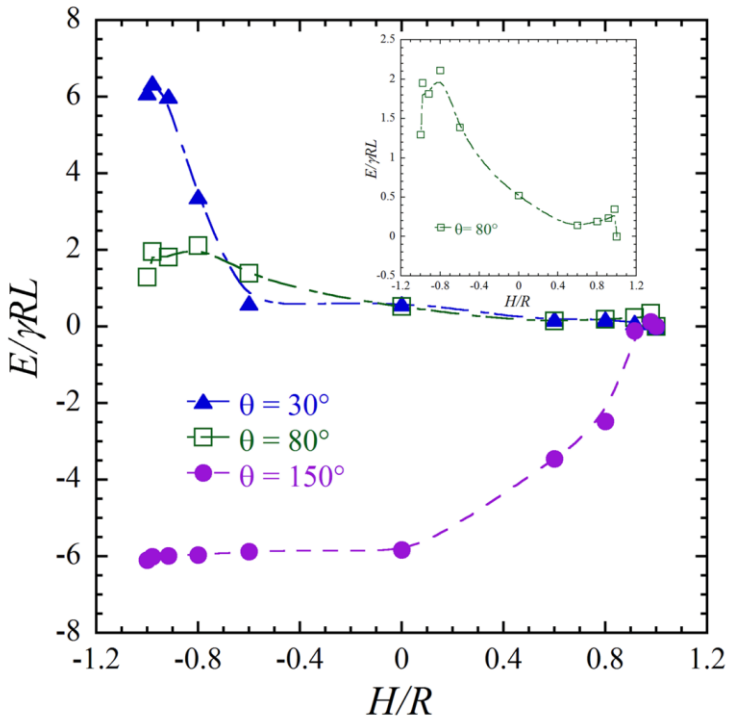

Figure 8 – Interfacial energy of hollow cylinders as a function of *H/R* for contact angles θ = 30, 80, and 150°.

below the interface at H/R = 1.0, where water prefers to fill the inside of the cylinder. In the case of 80° contact angle, we see a metastable state in which the cylinder prefers to sit on top of the interface at H/R = -1.0, as water does not get into the hollow cylinder. In this case however, if the cylinder is pushed under the water, it adopts a new equilibrium position at H/R = 1.0 as shown in the inset in figure 8.

Homogeneous hollow cylinders experience two different variations of interface deformation depending on their contact angle. For a cylinder sitting on top of the interface, there is a rise in the interface at the sides and a depression at the front and back, as shown in figure 9(a). When the cylinder is below the interface, the opposite occurs; the interface rises on the front/back and depresses on the sides, as shown in figure 7(b).

For two approaching homogeneous hollow cylinders, the capillary energy is characterized as a function of aspect ratio and position with respect to the interface. The contact angle is set to 80°, the height with respect to the interface is H/R = -1.0 and 1.0, and aspect ratio of 2.5 and 5. The results are shown figure 10. For cylinders of similar aspect ratio and separation distance(d_{cc}), the pair with H/R = -1.0 have a greater attraction for each other. For cylinders of similar H/R at the same d_{cc}, the pair of larger AR has a greater attraction, due to a larger deformation in the interface. The preferred orientation of two homogeneous hollow cylinders as they rotate about each other within the interfacial plane is determined for aspect ratio of AR = 5, contact angles of 80 and 150°, and the height of the cylinder with respect to the interface of H/R = -1.0. We vary ϕ in a range from 0 (side-by-side) to 180 (tip-to-tip), and at each angle, the cylinders are just touching each other. We note that hollow cylinders prefer side-by-side arrangement, until capillary energy overcomes the barrier (ΔE, figure 11) after which tip-to-tip orientation

becomes favorable. This barrier exists around $\phi \sim 140-150°$ for both hydrophilic and hydrophobic cylinders.

a.

b.

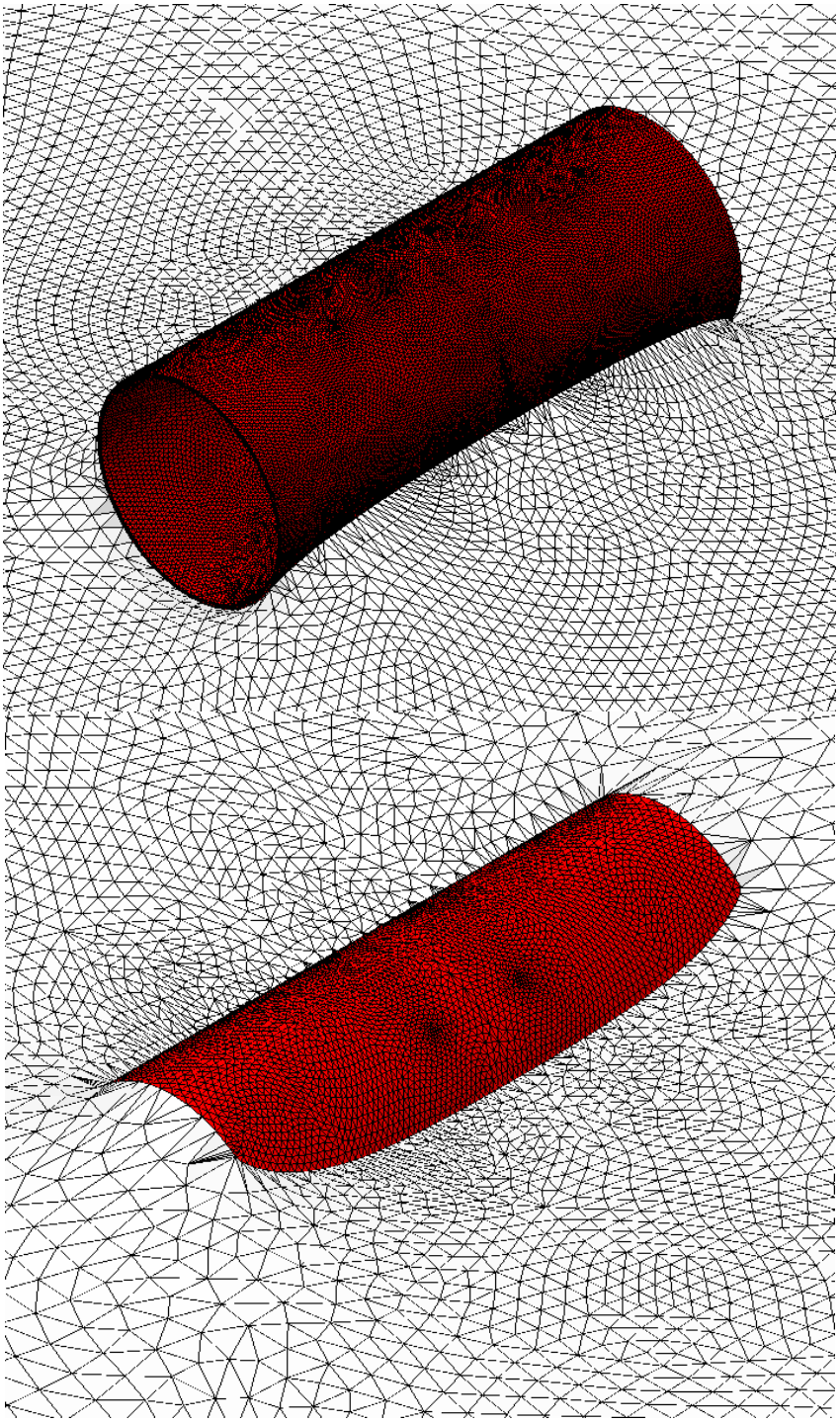

Figure 9 – Interface deformation for a homogeneous hollow cylinder of contact 80° on top (a) and below (b) of the interface.

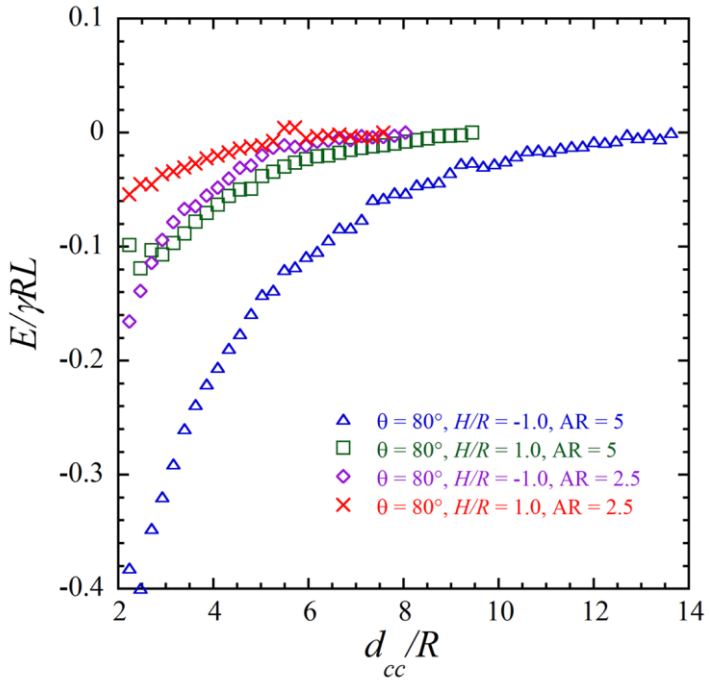

Figure 10 – Capillary energy vs. spacing for homogeneous hollow cylinders with contact angle θ = 80°, AR = 2.5 and 5, and H/R = 1.0 and -1.0.

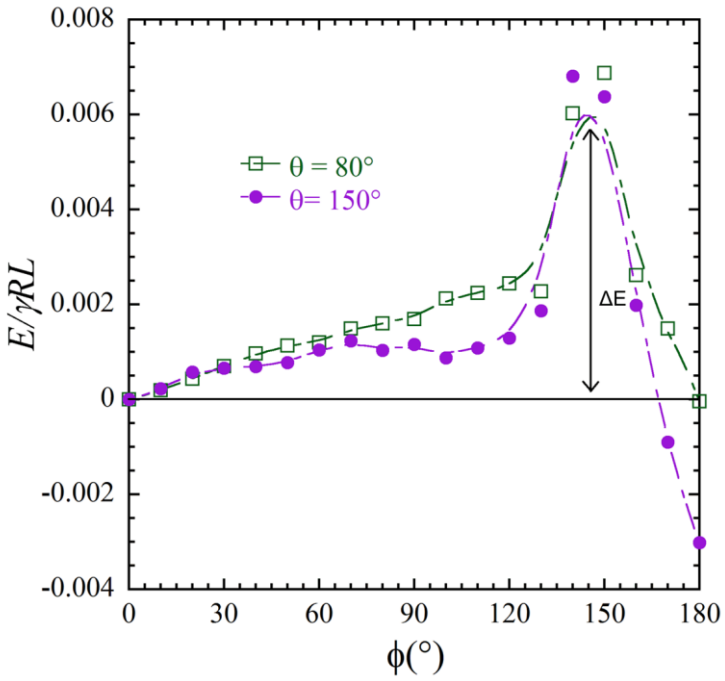

Figure 11 – Preferred in-plane orientation of a pair of homogenous hollow cylinders with contact angle θ = 80 and 150°, AR = 5, and *H/R* = -1.0.

Chapter 4

Solid Homogeneous Cylinders

4. Solid Homogeneous Cylinders

To compare the behavior of hollow homogeneous cylinders with their solid counterparts we investigate the preferred orientation of homogeneous solid cylinders. Similar to the hollow homogeneous cylinders, we vary the orientation angle as well as the aspect ratio for three different contact angles θ = 30, 80, and 150°. As shown in figure 12, solid homogeneous cylinders behave very similarly to their hollow counterparts. For

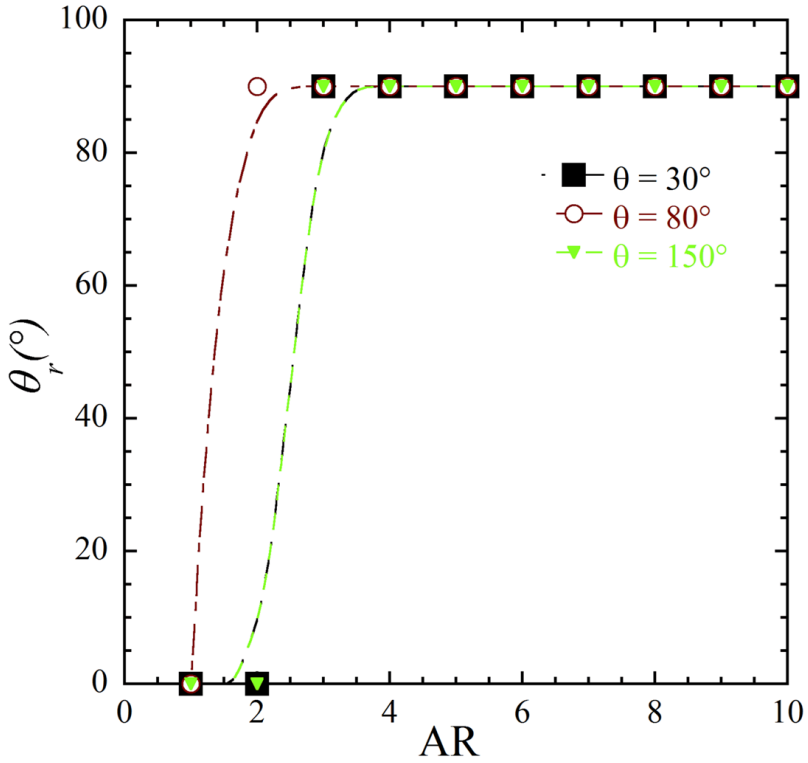

Figure 12 – Orientation of solid homogeneous cylinder as a function of aspect ratio for contact angles θ = 30, 80, and 150°.

small aspect ratios of ≤ 2, cylinders with contact angles θ = 30 and 150° prefer a vertical orientation, and for aspect ratios larger than 2, they prefer a horizontal orientation. For contact angle θ = 80° and an aspect ratio of 1, the cylinder prefers to sit vertically. At aspect ratios AR > 1, they prefer a horizontal orientation.

We compare the interface deformation and *H/R* of hollow cylinders with respect to the interface with their solid counterparts. When both hollow and solid cylinders are hydrophilic, they experience similar interface deformation; there is an interfacial rise in the front and back, and a depression on the sides, as shown in figure 13. For hydrophobic cylinders, the interfacial deformation is the opposite. The *H/R* of solid cylinders is initially set to 0. The solid cylinder simulations can move with respect to the interface until it reaches it preferred position.

The capillary energy between a pair of solid homogeneous cylinders and the preferred in-plane orientation is investigated. For cylinders with aspect ratio of AR = 5 and contact angle of 80°. This aspect ratio was chosen to ensure that the solid homogeneous cylinders are positioned parallel to the interface. The results of the

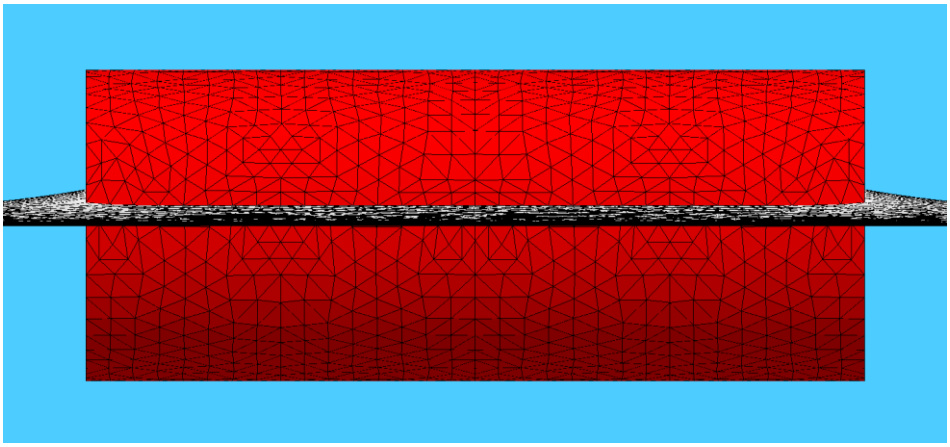

Figure 13 – Interface deformation of a single homogeneous solid cylinder with contact angle θ = 80° and aspect ratio AR = 5.

capillary energy as a function of their distance is shown in figure 14 (a). The capillary energy shows that the two cylinders attract each other. The preferred in-plane orientation results are shown in figure 14(b). A pair of solid homogeneous cylinders clearly prefers the tip-to-tip orientation. This is in contrast to a pair of hollow homogeneous cylinders as they could orient as tip-to-tip or side-by-side.

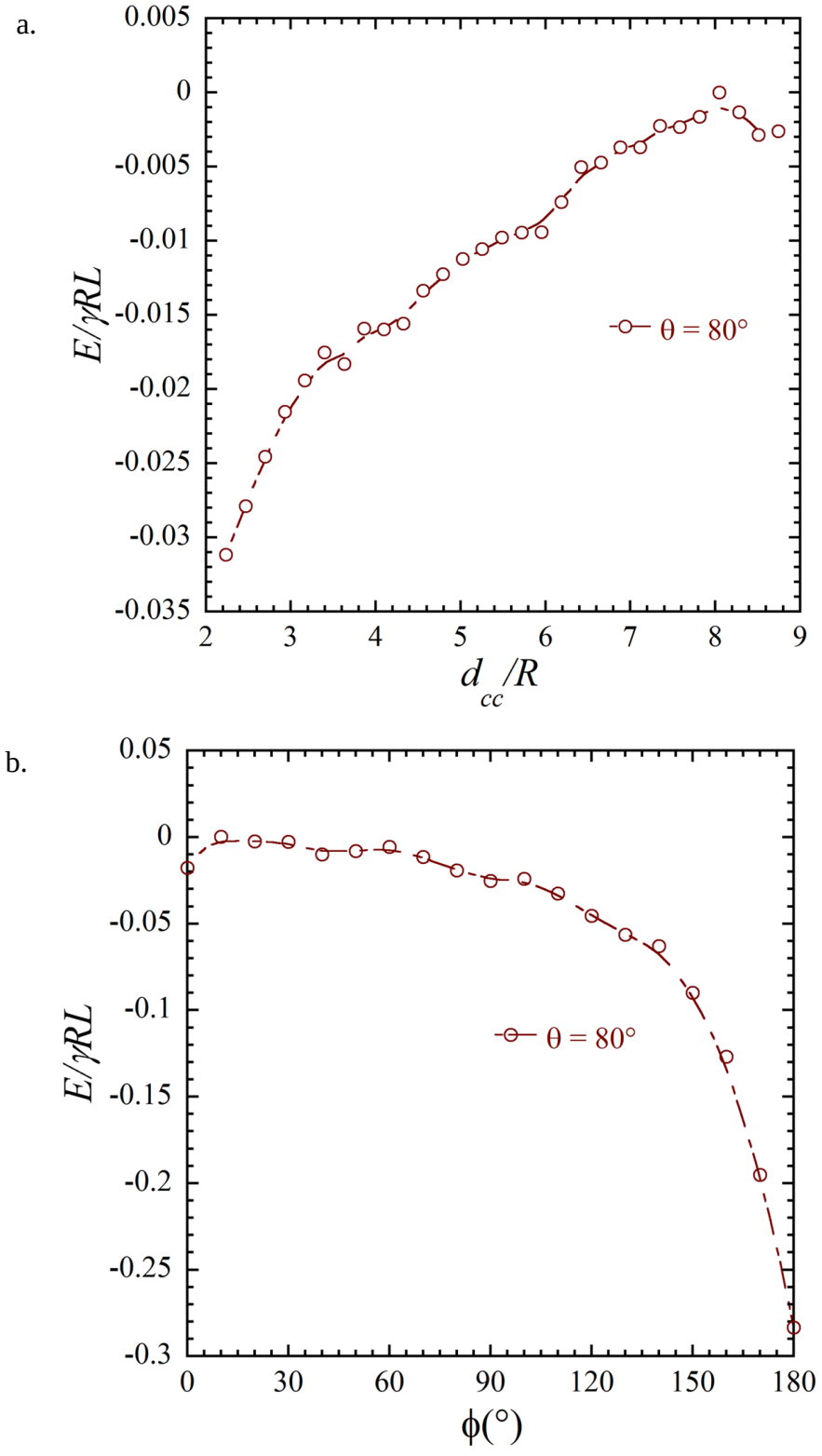

Figure 14 – (a) Capillary energy for two interacting homogeneous solid cylinders with contact angle θ = 80°, AR = 5, and *H/R* = 0. (b) Preferred orientation of a pair of homogenous solid cylinders with contact angle θ = 80°, AR = 5, and *H/R* = 0.

Chapter 5

Hollow Janus Cylinders

5. Hollow Janus Cylinders

Having investigated hollow and solid homogeneous cylinders, we now turn our attention to hollow Janus cylinders. First, we will investigate the preferred equilibrium orientation of a single hollow Janus cylinder. The cylinder is rotated around the *y*-axis (figure 15). We vary the aspect ratio from AR = 1 to 10, the rotation angle $\theta_{r,}$ from horizontally aligned along the interface to sitting perpendicular to it, and the amphiphilicity β = 10, 15, and 20°. The preferred orientation changes with amphiphilicity, from an orientation parallel to the interface (θ_r = 90°) for β = 10° to θ_r = 0° for higher β values as shown in figure 16. We observe that the preferred orientation is

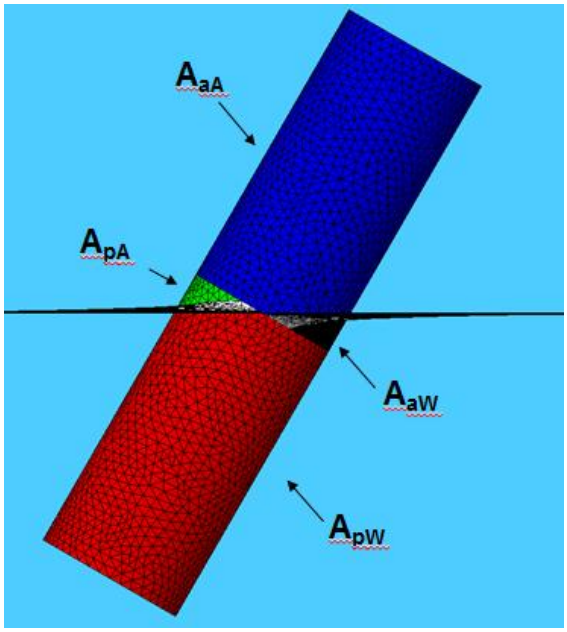

Figure 15 – Hollow Janus cylinder tilted about the interface with orientation angle θ_r = 0°, aspect ratio AR = 5, and amphiphilicity β= 30°.

sensitive to the aspect ratio at AR = 2 for amphiphilicty of β = 15°. As β increases, the affinity of hydrophilic and hydrophobic sides of the cylinder to be wet by their favorite fluids increases, explaining why θ_r = 0° is preferred at higher β values. Interface deformation around a single hollow Janus cylinder when the orientation is parallel to the interface (θ_r = 90°) is shown in figure 20.

The interface deformation around hollow Janus cylinders is shown in figure 17. Hollow Janus cylinders experience similar interface deformations when they are sitting on top of the interface at *H/R* = -1.0. On the sides of the cylinders where the surface is hydrophilic, the interface experiences a rise, and on the hydrophobic surface the interface experiences a depression. On the front and the back of the cylinder, regardless of whether it is hydrophobic or hydrophilic, the interface experiences a depression. We vary the position of the hollow Janus cylinder with respect to the interface, using an aspect ratio of AR = 5 and amphiphilicities β = 10 and 15°. The results in figure 18 show that the

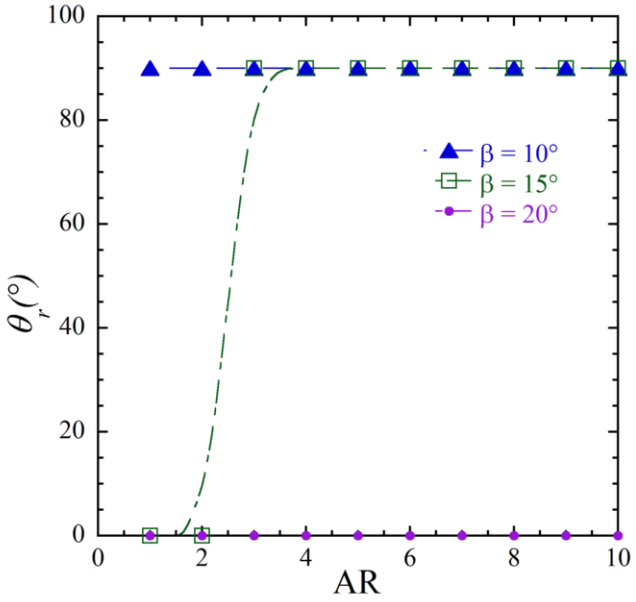

Figure 16 – Orientation with respect to the interface as a function of aspect ratio for single hollow Janus cylinders with amphiphilicity of β = 10, 15, and 20°.

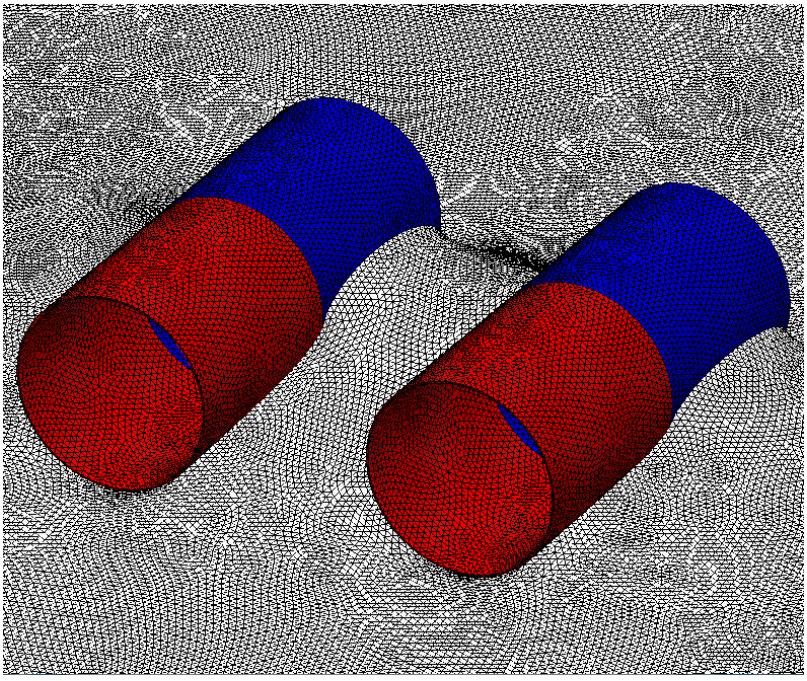

Figure 17 – Capillary bridge formed as a pair of hollow Janus cylinders with amphiphilicity β = 30°, are attracting each other. Blue corresponds to the hydrophilic portion of the particles.

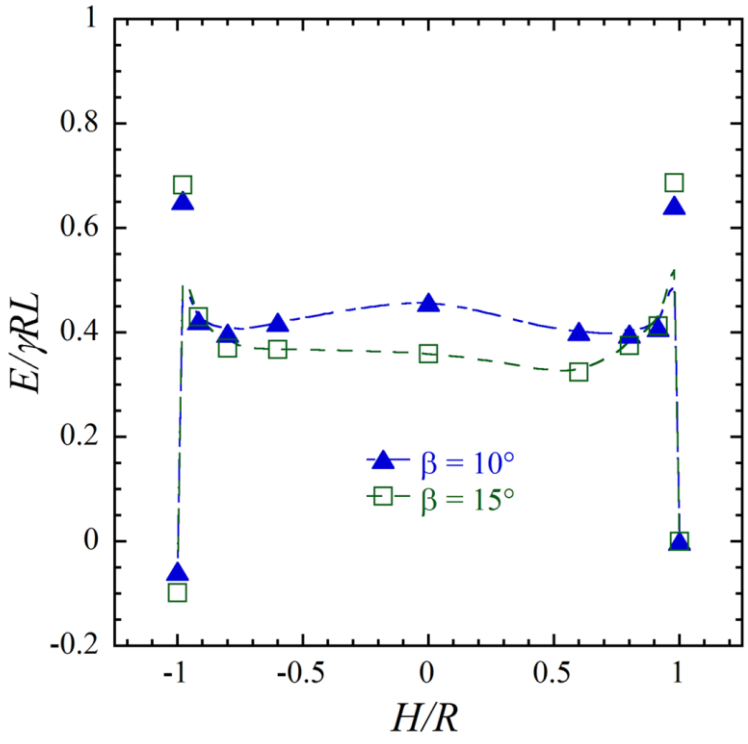

Figure 18 – Interfacial energy of a single hollow Janus cylinder as a function of *H/R* for amphiphilicities β = 10 and 15°.

cylinders prefer to either sit on top of the interface at H/R = -1.0 and not have the inside wetted, or to be completely submerged under the interface at H/R = 1.0 and have the inside filled with water.

The capillary energy between a pair of hollow Janus cylinders with an aspect ratio of AR = 5 and three different amphiphilicities of β = 10, 30, 50° is shown in figure 19. The cylinders are positioned at height H/R = -1.0 with respect to the interface. Evidently, the capillary attraction is stronger for Janus cylinders of higher amphiphilicity as they approach each other.

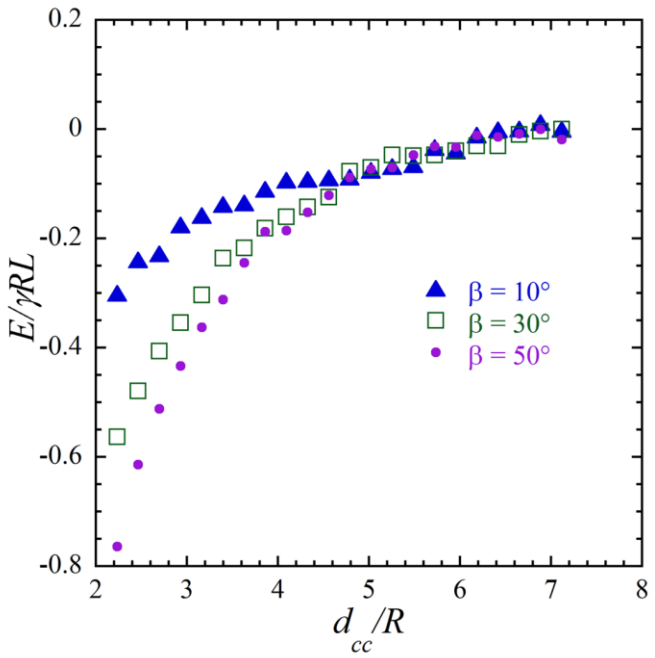

Figure 19 – The capillary energy vs. spacing between two hollow Janus cylinders with amphiphilicities β = 10, 30, and 50°.

To determine the preferred assembly orientation of a pair of hollow Janus cylinders, we have calculated the capillary energy as a function of angle ϕ (see figure 6). The cylinders have an aspect ratio of 5, height with respect to the interface of H/R = -1.0, and four amphiphilicities of β = 10, 15, 30, and 50°. As demonstrated in figure 21, for

higher amphiphilicity of β = 30° and 50° the cylinders prefer a side-by-side orientation, ϕ = 0. When amphiphilicity is decreased to β = 10 and 15°, the cylinders show equal preference to side-by-side (ϕ = 0) as they do to tip-to-tip (ϕ = 180) orientation. The interface deformation around the hollow Janus cylinders is shown in figure 22. This is consistent with the case of two homogeneous hollow cylinders, where side-by-side and tip-to-tip orientations have equal preference.

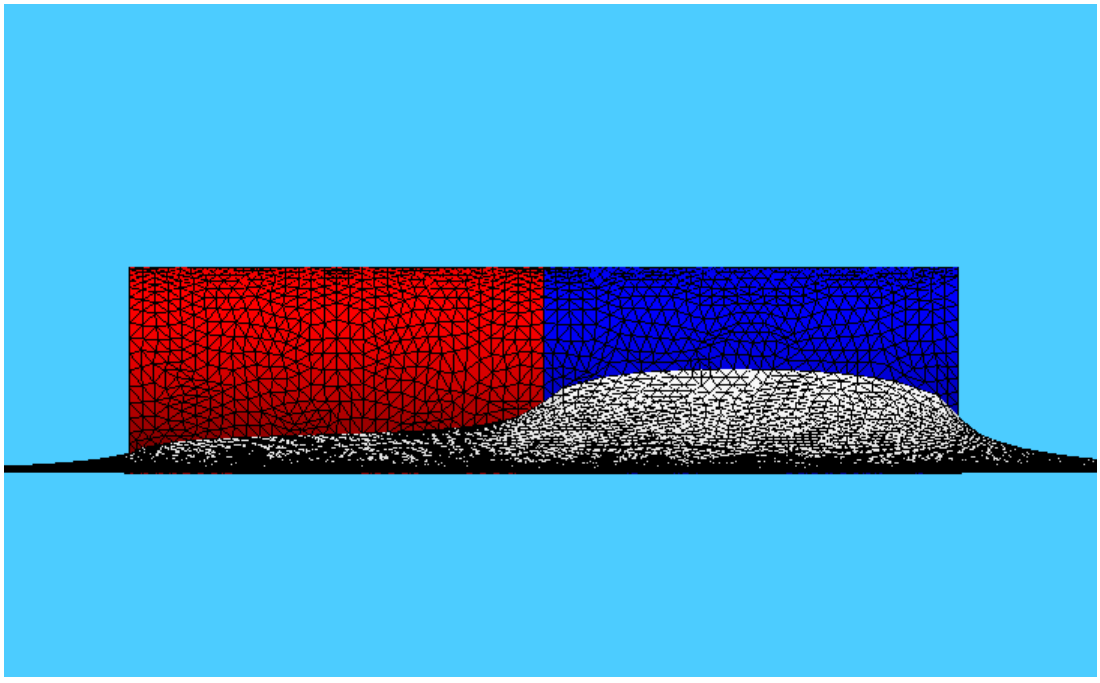

Figure 20 – Interface deformation around a single hollow Janus cylinder with amphiphilicity β = 30° and aspect ratio AR = 8.

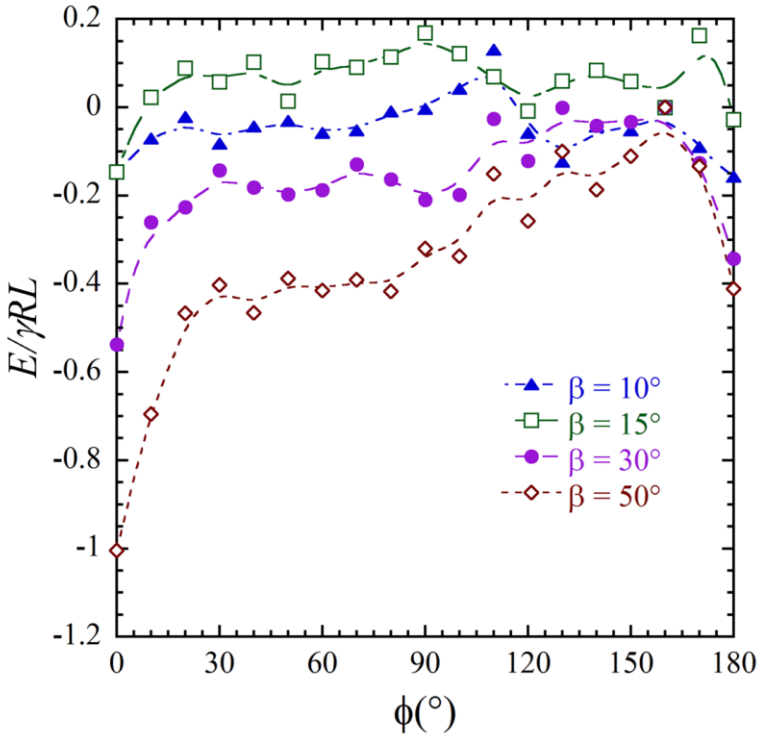

Figure 21 - Preferred in-plane orientation for a pair of hollow Janus cylinders with β = 10, 15, 30, and 50°, AR = 5, and *H/R* = -1.0.

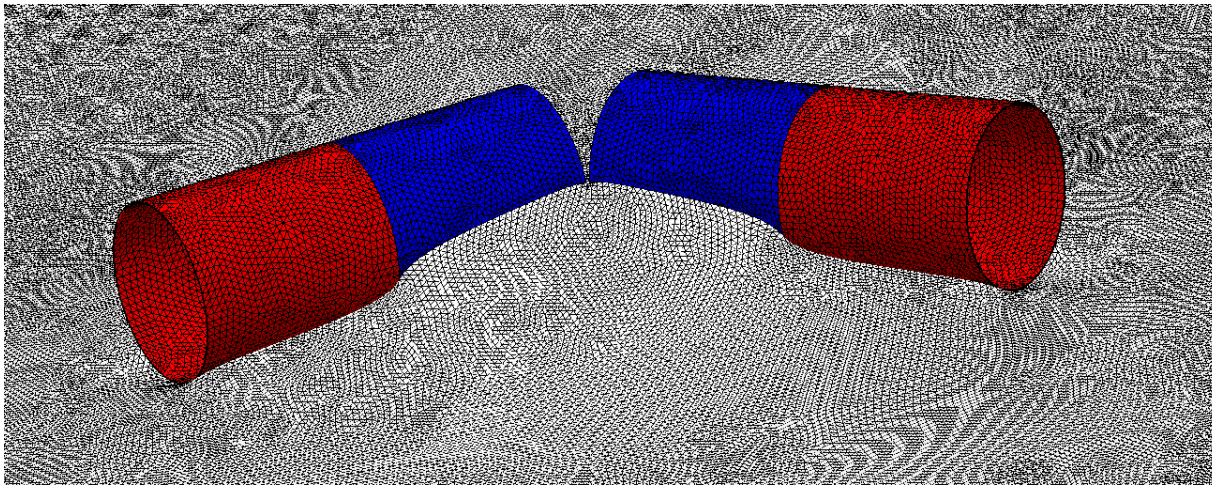

Figure 22 – Interface deformation around a pair of hollow Janus cylinders with amiphiphilicity b = 30°, aspect ratio AR = 5, and in-plane orientation angle ϕ = 120.

Chapter 6

Solid Janus Cylinders

6. Solid Janus Cylinders

We investigate the behavior of solid Janus cylinders to compare with hollow Janus ones. We begin by studying the preferred equilibrium orientation of a single solid Janus cylinder at an interface. We vary the aspect ratio and rotation angle θ_r discussed in the previous section. The amphiphilicity is tuned to β = 10, 30, and 50°. For amphiphilicity of β = 10°, when the aspect ratio AR is ≤ 2, the cylinder prefers a vertical

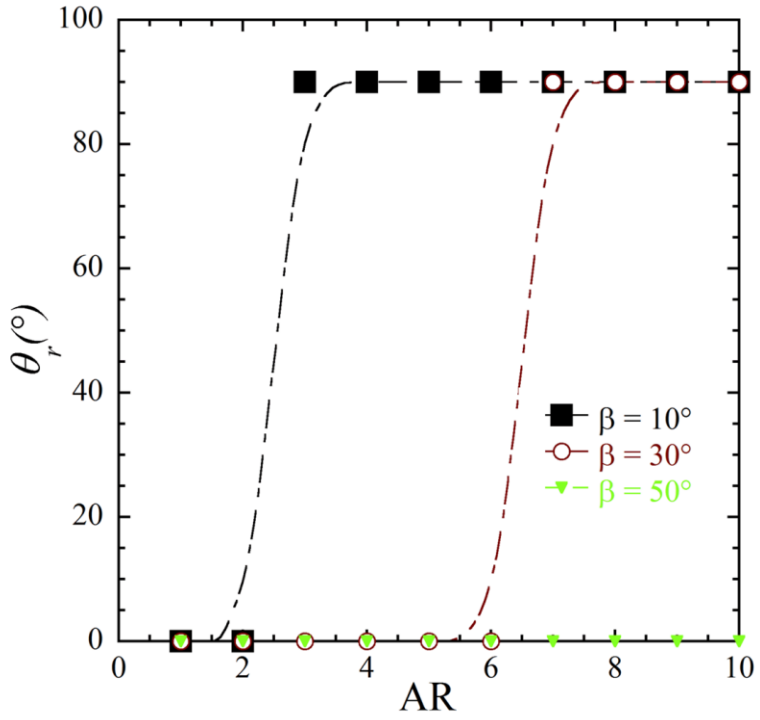

Figure 23 – Orientation with respect to the interface as a function of aspect ratio for a single solid Janus cylinder with amphiphilicity β = 10, 30, and 50°.

orientation (θ_r = 0°).For aspects ratios AR greater than or equal to 3, the cylinder prefers a horizontal orientation (θ_r = 90°). Amphiphilicity of β = 30° behaves in a similar manner, except it prefers a vertical orientation at aspect ratios < 6, and horizontal orientations at aspect ratios > 7. For amphiphilicity β = 50°, the cylinder always prefers vertical orientation, regardless of aspect ratio, as shown in figure 23. We note that solid Janus cylinders follow the same pattern as hollow Janus cylinders in that as the amphiphilicity increases, the cylinders prefer to take a vertical orientation to be wet

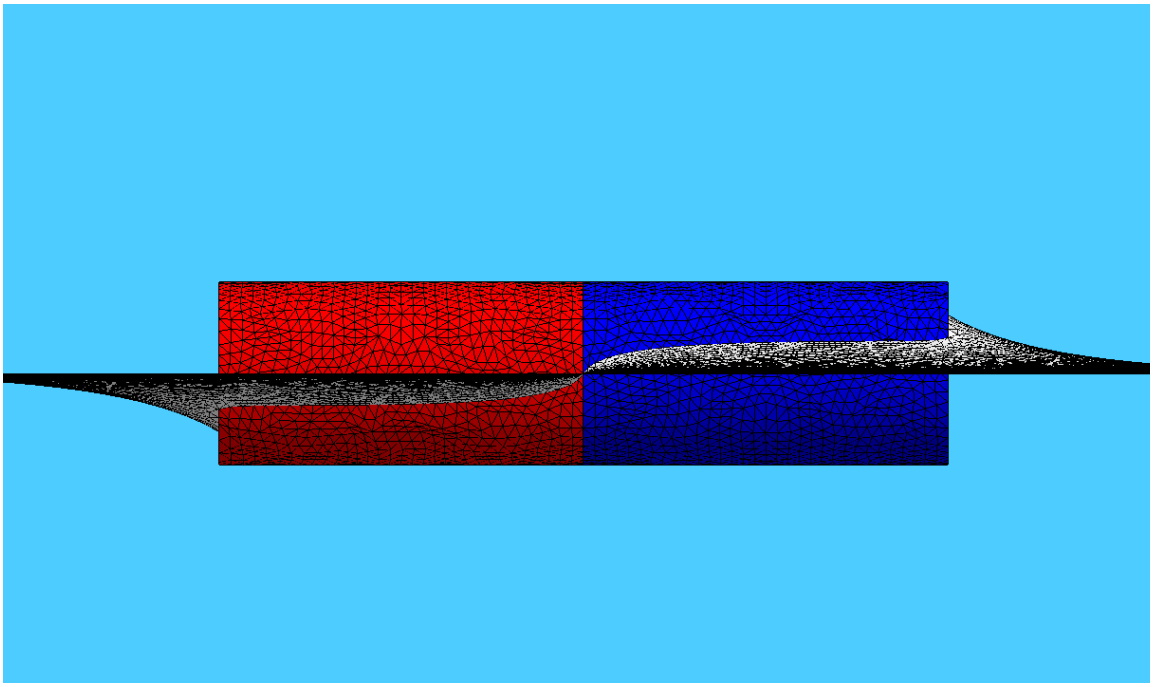

Figure 24 – Interface deformation around a single solid Janus cylinder with amphiphilicity β = 30° and aspect ratio AR = 8.

exposed to their favorite fluids. When solid Janus cylinders take a horizontal orientation (θ_r = 90°), the interface deforms in such a way that the sides and the front which are hydrophilic see a rise and the sides and the back which are hydrophobic see a depression, as shown in figure 24.

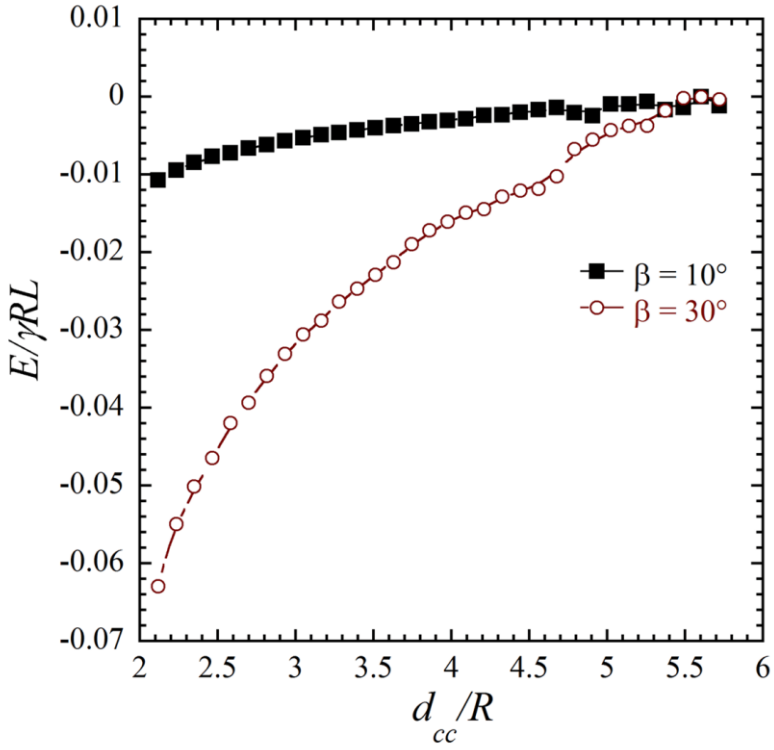

Figure 25 – The capillary energy vs. spacing between two solid Janus cylinders with amphiphilicities β = 10 and 30°.

The capillary interactions between a pair of solid Janus cylinders are studied. We use an aspect ratio of AR = 8 and amphiphiliticies of β = 10 and 30°, as this combination results in a horizontal orientation at the interface. The cylinders are initially placed at H/R = 0. Solid Janus cylinders with higher amphiliphicity have a larger attraction to each other, as shown in figure 25. These results are consistent with the capillary interactions exhibited by hollow Janus cylinders.

Finally, we determine the preferred in-plane assembly of a pair of solid Janus cylinders using the same approach used in previous sections. The cylinders have an aspect ratio of 8, initial height with respect to the interface of H/R = 0, and amphiphilicities of β = 10 and 30°. At lower amphiphillicities, when the cylinder is closer to a homogeneous one, solid Janus cylinders prefer tip-to-tip orientation (ϕ = 180). As the

amphiphilicity increases a side-by-side orientation (ϕ = 0) becomes the dominant orientation, as shown in figure 26. This preferred assembly of solid Janus cylinders is similar to that of hollow cylinders for large amphiphilicities, as they both greatly prefer a side-by-side orientation.

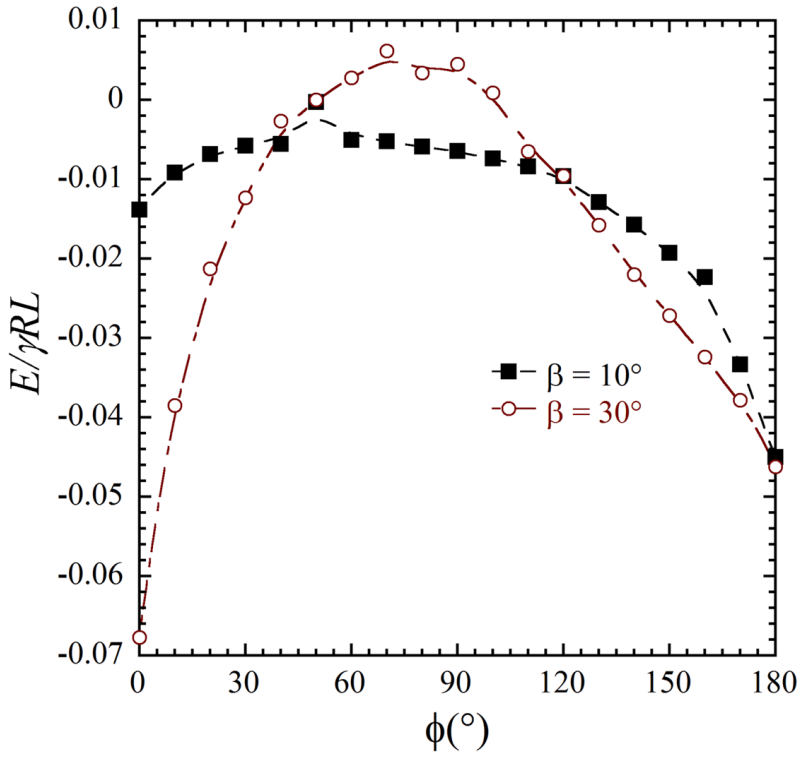

Figure 26 – Preferred in-plane orientation for a pair of solid Janus cylinders with β = 10 and 30°, AR = 8, and H/R = 0.

Chapter 7

Conclusions and Future Outlook

7. Conclusions and Future Outlook

We have investigated the interface deformation and interactions between hollow Janus cylinders at an air-water interface. We demonstrated for a single Janus cylinder the preferred orientation is dependent on amphiphilicity and aspect ratio. At low amphiphilicities, cylinders prefer a horizontal orientation (θ_r = 90°), and at larger amphiphilicites the cylinders prefer are vertical orientation (θ_r = 0°). The critical point at which hollow Janus cylinders change orientation from horizontal to vertical is at amphiphilicity β = 15°, and from aspect ratio AR = 2 to AR = 3.

For a pair of hollow Janus cylinders, the capillary energy is characterized as a function of varying positions with respect to the interface. As amphiphilicity is increased, the attraction between hollow Janus cylinders is increased as well. As these cylinders move further apart (d_{cc}/R > 3.5), it is clear that amphiphilicity does not affect their attraction to each other for a given aspect ratio and height of the cylinder with respect to the interface. The preferred orientation between hollow Janus cylinders as they rotate in a plane was also investigated. It was shown that as the amphiphilicity was increased, the hollow Janus cylinders experienced a greater affinity for side-by-side orientation. As the amphiphilicity is decreased and gets closer to homogeneous, the hollow Janus cylinders exhibit a similar preference to side-by-side as they do tip-to-tip orientation. Simulations of hollow homogeneous cylinders were used to confirm these results and showed that at a

contact angle of 80° these cylinders had similar preference as to those of small amphiphilicities in hollow Janus cylinders.

In the future, we plan to expand upon various aspects of our current work. Different variations of Janus cylinders will be studied, and the effect of asymmetry with respect to the Janus nature will be explored. Independently varying the amphiphilicites of the inside and outside of hollow cylinders as well as changing the patchiness along the length of the cylinders will provide further information about the dynamics of these particles. Finally, we plan to model cylinders of much smaller dimensions, incorporating forces that are significant at the nano-scale, to obtain insight regarding the effect of size on the self-assembly dynamics. These results would be relevant to various applications, such as the characterization of the interfacial behavior of carbon nanotubes. While this work has helped us develop an understanding of Janus cylinder behavior at an interface, additional simulations are necessary to improve upon this knowledge base and further the real-life applicability of this research.

8. References

1. Walther, A.; Mueller, A. H. E. Janus Particles: Synthesis, Self-Assembly, Physical Properties, and Applications. *Chemical Reviews* **2013,** *113* (7), 5194-5261.

2. Degennes, P. G. SOFT MATTER (NOBEL LECTURE). *Angewandte Chemie-International Edition in English* **1992,** *31* (7), 842-845.

3. Bhaskar, S.; Gibson, C. T.; Yoshida, M.; Nandivada, H.; Deng, X.; Voelcker, N. H.; Lahann, J. Engineering, Characterization and Directional Self-Assembly of Anisotropically Modified Nanocolloids. *Small* **2011,** *7* (6), 812-819.

4. Ding, H.-m.; Ma, Y.-q. Interactions between Janus particles and membranes. *Nanoscale* **2012,** *4* (4), 1116-1122.

5. Gkeka, P.; Sarkisov, L.; Angelikopoulos, P. Homogeneous Hydrophobic-Hydrophilic Surface Patterns Enhance Permeation of Nanoparticles through Lipid Membranes. *Journal of Physical Chemistry Letters* **2013,** *4* (11), 1907-1912.

6. Wang, F.; Pauletti, G. M.; Wang, J.; Zhang, J.; Ewing, R. C.; Wang, Y.; Shi, D. Dual Surface-Functionalized Janus Nanocomposites of Polystyrene/Fe3O4@SiO2 for Simultaneous Tumor Cell Targeting and Stimulus-Induced Drug Release. *Advanced Materials* **2013,** *25* (25), 3485-3489.

7. Bucaro, M. A.; Kolodner, P. R.; Taylor, J. A.; Sidorenko, A.; Aizenberg, J.; Krupenkin, T. N. Tunable Liquid Optics: Electrowetting-Controlled Liquid Mirrors Based on Self-Assembled Janus Tiles. *Langmuir* **2009,** *25* (6), 3876-3879.

8. Faria, J.; Ruiz, M. P.; Resasco, D. E. Phase-Selective Catalysis in Emulsions Stabilized by Janus Silica-Nanoparticles. *Advanced Synthesis & Catalysis* **2010,** *352* (14-15), 2359-2364.

9. Erhardt, R.; Boker, A.; Zettl, H.; Kaya, H.; Pyckhout-Hintzen, W.; Krausch, G.; Abetz, V.; Muller, A. H. E. Janus micelles. *Macromolecules* **2001,** *34* (4), 1069-1075.

10. Walther, A.; Goeldel, A.; Mueller, A. H. E. Controlled crosslinking of polybutadiene containing block terpolymer bulk structures: A facile way towards complex and functional nanostructures. *Polymer* **2008,** *49* (15), 3217-3227.

11. Walther, A.; Drechsler, M.; Rosenfeldt, S.; Harnau, L.; Ballauff, M.; Abetz, V.; Mueller, A. H. E. Self-Assembly of Janus Cylinders into Hierarchical Superstructures. *Journal of the American Chemical Society* **2009,** *131* (13), 4720-4728.

12. Walther, A.; Andre, X.; Drechsler, M.; Abetz, V.; Mueller, A. H. E. Janus discs. *Journal of the American Chemical Society* **2007,** *129* (19), 6187-6198.

13. Walther, A.; Drechsler, M.; Mueller, A. H. E. Structures of amphiphilic Janus discs in aqueous media. *Soft Matter* **2009,** *5* (2), 385-390.

14. Lattuada, M.; Hatton, T. A. Preparation and controlled self-assembly of janus magnetic nanoparticles. *Journal of the American Chemical Society* **2007,** *129* (42), 12878-12889.

15. Pradhan, S.; Xu, L.-P.; Chen, S. Janus nanoparticles by interfacial engineering. *Advanced Functional Materials* **2007,** *17* (14), 2385-2392.

16. Nie, L.; Liu, S.; Shen, W.; Chen, D.; Jiang, M. One-pot synthesis of amphiphilic polymeric Janus particles and their self-assembly into supermicelles with a narrow size distribution. *Angewandte Chemie-International Edition* **2007,** *46* (33), 6321-6324.

17. Isojima, T.; Lattuada, M.; Vander Sande, J. B.; Hatton, T. A. Reversible clustering of pH- and temperature-responsive Janus magnetic nanoparticles. *Acs Nano* **2008,** *2* (9), 1799-1806.

18. Zana, R. Dimeric and oligomeric surfactants. Behavior at interfaces and in aqueous solution: a review. *Advances in Colloid and Interface Science* **2002,** *97* (1-3), 205-253.

19. Zeng, C.; Brau, F.; Davidovitch, B.; Dinsmore, A. D. Capillary interactions among spherical particles at curved liquid interfaces. *Soft Matter* **2012,** *8* (33), 8582-8594.

20. Binks, B. P.; Fletcher, P. D. I. Particles adsorbed at the oil-water interface: A theoretical comparison between spheres of uniform wettability and "Janus" particles. *Langmuir* **2001,** *17* (16), 4708-4710.

21. Pieranski, P. TWO-DIMENSIONAL INTERFACIAL COLLOIDAL CRYSTALS. *Physical Review Letters* **1980,** *45* (7), 569-572.

22. Oettel, M.; Dominguez, A.; Dietrich, S. Effective capillary interaction of spherical particles at fluid interfaces. *Physical Review E* **2005,** *71* (5).

23. Ghezzi, F.; Earnshaw, J. C. Formation of meso-structures in colloidal monolayers. *Journal of Physics-Condensed Matter* **1997,** *9* (37), L517-L523.

24. Ghezzi, F.; Earnshaw, J. C.; Finnis, M.; McCluney, M. Pattern formation in colloidal monolayers at the air-water interface. *Journal of Colloid and Interface Science* **2001,** *238* (2), 433-446.

25. Ruiz-Garcia, J.; Gamez-Corrales, R.; Ivlev, B. I. Formation of two-dimensional colloidal voids, soap froths, and clusters. *Physical Review E* **1998,** *58* (1), 660-663.

26. Ruiz-Garcia, J.; Ivlev, B. I. Formation of colloidal clusters and chains at the air/water interface. *Molecular Physics* **1998,** *95* (2), 371-375.

27. Stamou, D.; Duschl, C.; Johannsmann, D. Long-range attraction between colloidal spheres at the air-water interface: The consequence of an irregular meniscus. *Physical Review E* **2000,** *62* (4), 5263-5272.

28. Botto, L.; Yao, L.; Leheny, R. L.; Stebe, K. J. Capillary bond between rod-like particles and the micromechanics of particle-laden interfaces. *Soft Matter* **2012,** *8* (18), 4971-4979.

29. Pozrikidis, C. Capillary attraction of floating rods. *Engineering Analysis with Boundary Elements* **2012,** *36* (5), 836-844.

30. Cooray, H.; Cicuta, P.; Vella, D. The capillary interaction between two vertical cylinders. *Journal of Physics-Condensed Matter* **2012,** *24* (28).

31. Raufaste, C.; Cox, S. Deformation of a free interface pierced by a tilted cylinder: Variation of the contact angle. *Colloids and Surfaces a-Physicochemical and Engineering Aspects* **2013,** *438*, 126-131.

32. Hunter, T. N.; Pugh, R. J.; Franks, G. V.; Jameson, G. J. The role of particles in stabilising foams and emulsions. *Advances in Colloid and Interface Science* **2008,** *137* (2), 57-81.

33. Aveyard, R. Can Janus particles give thermodynamically stable Pickering emulsions? *Soft Matter* **2012,** *8* (19), 5233-5240.

34. Glotzer, S. C.; Solomon, M. J. Anisotropy of building blocks and their assembly into complex structures. *Nature Materials* **2007,** *6* (8), 557-562.

35. Rezvantalab, H.; Shojaei-Zadeh, S. Capillary interactions between spherical Janus particles at liquid-fluid interfaces. *Soft Matter* **2013,** *9* (13), 3640-3650.

36. Binks, B. P. Particles as surfactants - similarities and differences. *Current Opinion in Colloid & Interface Science* **2002,** *7* (1-2), 21-41.

37. Casagrande, C.; Fabre, P.; Raphael, E.; Veyssie, M. JANUS BEADS - REALIZATION AND BEHAVIOR AT WATER OIL INTERFACES. *Europhysics Letters* **1989,** *9* (3), 251-255.

38. Casagrande, C.; Veyssie, M. JANUS BEADS - REALIZATION AND 1ST OBSERVATION OF INTERFACIAL PROPERTIES. *Comptes Rendus De L Academie Des Sciences Serie Ii* **1988,** *306* (20), 1423-1425.

39. Hirose, Y.; Komura, S.; Nonomura, Y. Adsorption of Janus particles to curved interfaces. *Journal of Chemical Physics* **2007,** *127* (5).

40. Ondarcuhu, T.; Fabre, P.; Raphael, E.; Veyssie, M. SPECIFIC PROPERTIES OF AMPHIPHILIC PARTICLES AT FLUID INTERFACES. *Journal De Physique* **1990,** *51* (14), 1527-1536.

41. Park, B. J.; Lee, D. Equilibrium Orientation of Nonspherical Janus Particles at Fluid-Fluid Interfaces. *Acs Nano* **2012,** *6* (1), 782-790.

42. Park, B. J.; Choi, C.-H.; Kang, S.-M.; Tettey, K. E.; Lee, C.-S.; Lee, D. Geometrically and chemically anisotropic particles at an oil-water interface. *Soft Matter* **2013,** *9* (12), 3383-3388.

43. Brakke, K. A. The surface evolver and the stability of liquid surfaces. *Philosophical Transactions of the Royal Society a-Mathematical Physical and Engineering Sciences* **1996,** *354* (1715), 2143-2157.

44. Rezvantalab, H.; Shojaei-Zadeh, S. Role of Geometry and Amphiphilicity on Capillary-Induced Interactions between Anisotropic Janus Particles. *Langmuir* **2013,** *29* (48), 14962-14970.